Measurements of electroweak penguin and leptonic $B_{(s)}$ decays at Belle

Felicitas Andrea Breibeck[*]

Institute of High Energy Physics, Austrian Academy of Science
E-mail: Felicitas.Breibeck@oeaw.ac.at

We present the results of the angular analysis for $B^0 \to K^*(892)^0 \ell^+ \ell^-$ using the full Belle data sample corresponding to an integrated luminosity of $711\,\mathrm{fb}^{-1}$. The obtained results are in agreement with the latest LHCb analyses and show a $2.1\,\sigma$ deviation from the DHMV Standard Model prediction in the range $4.0\,\mathrm{GeV}^2 < q^2 < 8.0\,\mathrm{GeV}^2$.

Furthermore we introduce a hadronic tagging procedure for B_s^0 mesons in the Belle $\Upsilon(5S)$ data sample that will open the opportunity to study leptonic and semi-leptonic B_s^0 final states in future analyses.

38th International Conference on High Energy Physics
3-10 August 2016
Chicago, USA

---

[*]Speaker.

1. Introduction

The Belle experiment, located at the asymmetric e^+e^- collider KEK-B [1] in Tsukuba Japan, has collected an integrated luminosity of $711\,\text{fb}^{-1}$ at the $\Upsilon(4S)$ resonance and $121.4\,\text{fb}^{-1}$ at the $\Upsilon(5S)$ resonance. The latter is a unique data sample at B factories and provides the opportunity to study decays of B_S^0 mesons.

The Belle detector (see fig. 1) is a large-solid-angle magnetic spectrometer that consists of a silicon vertex detector (SVD), a 50-layer central drift chamber (CDC), an array of aerogel threshold Cherenkov counters (ACC), a barrel-like arrangement of time-of-flight scintillation counters (TOF), and an electromagnetic calorimeter comprised of CsI(Tl) crystals (ECL) located inside a super-conducting solenoid coil that provides a 1.5 T magnetic field. An iron flux-return located outside of the coil is instrumented to detect K_L^0 mesons and to identify muons (KLM). The detector is described in detail elsewhere [2].
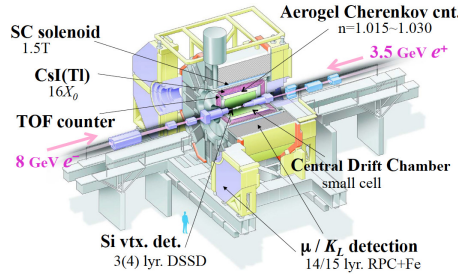

Figure 1: A schematic view of the Belle detector including its main sub-detector system.

2. Angular analysis of $B^0 \to K^*(892)^0 \ell^+ \ell^-$

Figures 2 (a), (b) and (c) illustrate the Standard Model (SM) Feynman diagrams for the rare decays $B^0 \to K^*(892)^0 \ell^+ \ell^-$ with $\ell = e, \mu$, where the $b \to s$ quark transition is described by a penguin or box diagram, respectively. New Physics effects can enter through additional loop processes where new particles replace the SM $W^\pm$ bosons in the box diagrams as shown in figure 2 (d), thus altering the branching ratios of these decay modes. In addition, angular observables describing the differential decay rate of these processes can be influenced by various extensions of the SM, e.g. models with minimal flavor violation, general minimal supersymmetric Standard Models and flavor-blind minimal supersymmetric Standard Models [3, 4].

Previously the decay $B^0 \to K^*(892)^0 \ell^+ \ell^-$ has been studied by the Belle, BaBar and CDF collaborations [5, 6, 7]. However, the LHCb experiment was the first one to publish a full angular analysis for the $B^0 \to K^*(892)^0 \mu^+ \mu^-$ decay mode [8, 9]. Their results are especially interesting, as LHCb observed a $3.4\,\sigma$ deviation from the SM prediction in the P_5' angular observable [10].

The currently ongoing study performed by Belle [11] investigates both $B^0 \to K^*(892)^0 \ell^+ \ell^-$ channels (with $\ell = e, \mu$) and thus adds the electron mode to the angular analysis. The reconstruction process requires that all charged tracks originate within $|dr| < 1.0\,\text{cm}$ in radial direction and $|dz| < 5.0\,\text{cm}$ in beam direction with respect to the interaction point. The particle identification
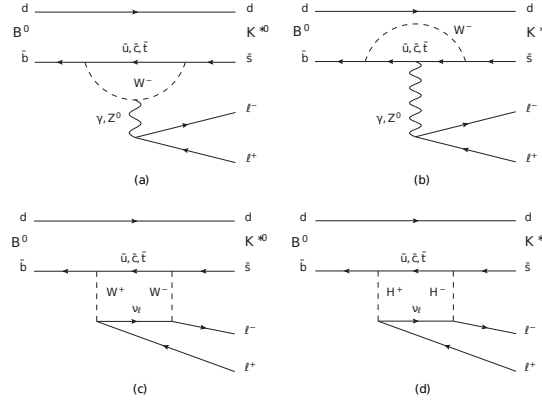
Figure 2: Standard model penguin and *W* box diagrams are presented in plots (a), (b) and (c) while plot (d) illustrates a box diagram including charged Higgs bosons.

for charged hadrons, namely $\pi^\pm$ and $K^\pm$, is based on the combined information of the CDC, TOF and ACC, while the electron identification additionally uses the ECL measurements and muons are identified using the KLM system. The $K^*(892)^0$ meson is reconstructed in the $K^*(892)^0 \to K^+\pi^-$ final state, where the invariant mass has to lie within $0.6\,\text{GeV} < M_{K^*} < 1.4\,\text{GeV}$.

Due to the special 2-body kinematic in $e^+e^- \to \Upsilon(4S) \to B\bar{B}$ events the signal yield can be extracted using two independent kinematic variables ΔE and M_{bc}:

$$\Delta E = E_B^* - E_{beam}^* \qquad \text{and} \qquad M_{bc} = \sqrt{E_{beam}^2 - (p_B^*)^2} \tag{2.1}$$

where E_{beam}^* is the beam energy in the center of mass frame and E_B^* and p_B^* denote the energy and the momentum of the reconstructed B_s^0 meson, respectively, given in the center of mass system. The allowed energy ranges for this reconstruction are $-0.1\,(-0.05)\,\text{GeV} < \Delta E < 0.05\,\text{GeV}$ for $\ell = e$ ($\ell = \mu$) and $5.22\,\text{GeV} < M_{bc} < 5.3\,\text{GeV}$.

Important background sources are decays from $J/\psi \to \ell^+\ell^-$ and $\psi(2S) \to \ell^+\ell^-$ mimicing the signal which is vetoed by applying selections on the reconstructed di-lepton mass $M_{\ell^+\ell^-}$. To further suppress background neural networks are sequentially included during the reconstruction.

The differential decay rate is described by three angles [8]:

- θ_l: angle between direction of ℓ^+ (ℓ^-) and opposite direction of B ($\bar{B}$) in rest frame of di-lepton system

- θ_k: angle between direction of kaon and opposite direction of B ($\bar{B}$) in K^* rest frame

- ϕ: angle between decay plane formed by $\ell^+\ell^-$ and K^* decay plane

In order to complete a full angular analysis it is necessary to perform an eight-dimensional fit. As the available statistic is not high enough for such a fit, a folding technique [9, 12, 13] is used applying variable transformations and use the symmetries of the sine and cosine functions to cancel several terms in the calculation of the differential decay rate. Thus, the number of free parameters
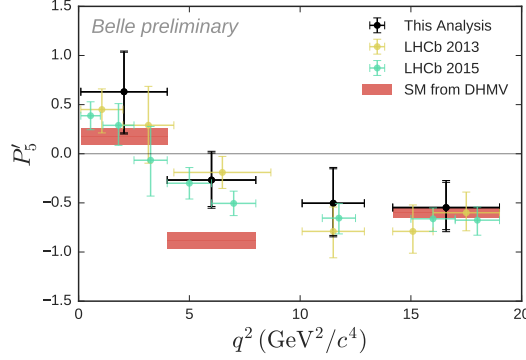
2

Figure 3: Results regarding the P'_5 observable are shown as black crosses and are in agreement with the LHCb results. The SM prediction based on DHMV is indicated as red bar.

can be reduced to three: the longitudinal polarization F_L of the K^* meson, S_3 and the respective S_i or P'_i observable which is determined by the fit.

Figure 3 presents the obtained results for the angular observable P'_5 in dependence of $q^2 = M^2_{\ell^+\ell^-}$ where a 2.1σ deviation from the DHMV [14, 15] Standard Model prediction is found in the range $4.0\,\mathrm{GeV}^2 < q^2 < 8.0\,\mathrm{GeV}^2$.

3. The B_s^0 hadronic tag

While the Belle experiment has been very successful in studying hadronic B_s^0 decay modes [16, 17], leptonic and semi-leptonic decays are much more challenging due to the undetectable neutrinos in the final states. In these case the information on the neutrino momentum and energy is lost and thus the kinematic of these events cannot be resolved resulting in background that is order of magnitudes higher compared to hadronic final states. The amount of background can be significantly reduced by applying a hadronic tagging procedure as illustrated in figure 4 where one $B_{(s)}$ meson is reconstructed in a fully hadronic final state, the so-called tag side, while the second $B_{(s)}$ is reconstructed in the signal decay to be searched. This method has already been used successfully for several analyses [18, 19, 20]. However, up to today only a hadronic tag including $B^\pm$ and B^0 decays has been available.

In order to open the opportunity to study $B_s \to \tau^+\tau^-$ and other leptonic and semi-leptonic B_s^0 decays, a hadronic tag has been currently developed for the Belle $\Upsilon(5S)$ data sample. This software reconstructs more than 5000 exclusive B_s^0 decay modes using a hierarchical architecture which consists of four stages. In a first step charged tracks are identified as either $e^\pm$, $\mu^\pm$, $\pi^\pm$ or $K^\pm$, while γ candidates are selected among the detected energy clusters in the ECL exceeding a certain energy threshold. Furthermore, K_S^0 mesons are reconstructed in the decay mode $K_S^0 \to \pi^+\pi^-$ and neutral pions in $\pi^0 \to \gamma\gamma$. During the second stage of the hadronic tag the charged tracks, γ, K_S^0 and π^0 candidates are combined to form light mesons, e.g. ω, ρ, ϕ, and the J/ψ meson, while the third stage reconstructs $D_{(s)}^{(*)}$ mesons. In the last step all previously identified and reconstructed particles are used to form B_s^0 candidates decaying into 2-body final states where M_{bc} is required to lie above
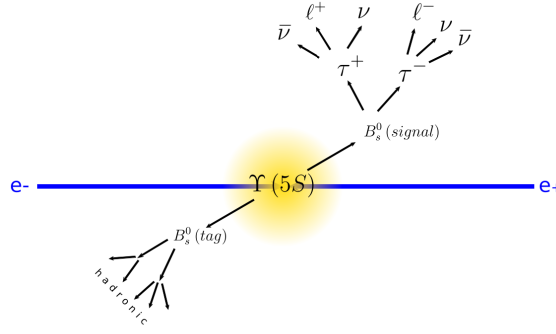
3

Figure 4: Schematic illustration of the hadronic tagging procedure. While one of the two B_s^0 mesons is reconstructed in a full hadronic final state, while the signal side decay, here $B_s \to \tau^+\tau^-$, is reconstructed from the remaining charged tracks.

5.2 GeV and ΔE within $-0.3\,\text{GeV} < \Delta E < 0.3\,\text{GeV}$.

In order to reduce the amount of background reconstructed in the hadronic B_s^0 tag more than 100 neural networks based on the NeuroBayes$^{\circledR}$ software were trained for every meson and each decay mode to distinguish correctly reconstructed particles from background events. The most important training variables are the likelihood ratios used for the identification of charged particles, the respective network output of the daughter particles and the energy difference ΔE. These networks are included in every stage of the reconstruction procedure. The selection criteria for the network output in the first and second stage have been optimized using a figure-of-merit procedure, while the threshold applied on the network output obtained for the $D_{(s)}^{(*)}$ mesons is moderate. However, there is no limit regarding the network output for the B_s^0 decays as the desired purity of the tag side B_s^0 sample can depend on the signal side decay.

A preliminary estimation of the achieved efficiency ε is determined by performing an extended likelihood fit on the ΔE distribution in order to calculate the signal yield. The efficiency is defined as the ratio between the number of fitted events within the peaking signal component and all events that have been processed by the software. The preliminary results show an achieved efficiency of $\varepsilon = 0.68\%$.

4. Summary

We presented an angular analyses of the decay $B^0 \to K^*(892)^0 \ell^+\ell^-$ with $\ell = e$, μ using eight free parameters and a folding technique to reduce the number of parameters to three without losing experimental sensitivity. The results are in agreement with previously published LHCb studies and show a 2.1 σ deviation from the DHMV Standard Model prediction in the angular observable P_5' in the range $4.0\,\text{GeV}^2 < q^2 < 8.0\,\text{GeV}^2$.

In addition we introduced a B_s^0 hadronic tag for the Belle $\Upsilon(5S)$ data sample that uses a hierarchical architecture to reconstruct more than 5000 exclusive B_s^0 decays. Signal and background are distinguished applying more than 100 trained neural networks. The preliminary achieved efficiency is determined to be $\varepsilon = 0.68\%$.

Acknowledgments

References

[1] S. Kurokawa and E. Kikutani, Nucl. Instr. and. Meth. A 499, 1 (2003), and other papers included in this volume.

[2] A. Abashian *et al.* [Belle Collaboration], Nucl. Instr. and Meth. A **479**, 117 (2002).

[3] W. Altmannshofer *et al.*, JHEP 01, 019 (2009), arXiv:0811.1214 [hep-ph].

[4] A. Bartl *et al.*, Phys. Rev. D 64, 1098 (2001), arXiv:0103324 [hep-ph].

[5] J.-T. Wei *et al.* [Belle Collaboration], Phys. Rev. Lett. 103, 1161 (2009), arXiv:0904.0770 [hep-ex].

[6] B. Aubert *et al.* [BaBar Collaboration], Phys. Rev. D 79, 031102 (2009), arXiv:0804.4412 [hep-ex].

[7] T. Aaltonen *et al.* [CDF Collaboration], Phys. Rev. Lett. 108, 081807 (2012), arXiv:1108.0695 [hep-ex].

[8] R. Aaij *et al.* [LHCb Collaboration], JHEP 08, 131 (2013), arXiv:1304.6325 [hep-ex].

[9] R. Aaij *et al.* [LHCb Collaboration], Phys. Rev. Lett. 111, 191801 (2013), arXiv:1308.1707 [hep-ex].

[10] R. Aaij *et al.* [LHCb Collaboration], JHEP 02, 104 (2016), arXiv:1512.04442 [hep-ex].

[11] S. Wehle *et al.* [Belle Collaboration], arXiv:1612.05014 [hep-ex] (2016).

[12] S. Descotes-Genon, T. Hurth, J. Matias and J. Virto, JHEP 1305, 137 (2013), arXiv:1303.5794 [hep-ph].

[13] M. D. Cian, *Track Reconstruction Efficiency and Analysis of $B^0 \to K^{*0} \mu^+ \mu^-$ at the LHCb Experiment*, Ph.D. thesis, University of Zurich (2013).

[14] B. Capdevila, S. Descotes-Genon, J. Matias and J. Virto, JHEP 10, 075 (2016), arXiv:1605.03156 [hep-ph].

[15] S. Descotes-Genon, L. Hofer, J. Matias and J. Virto, JHEP 12, 125 (2014), arXiv:1407.8526 [hep-ph].

[16] F. Thorne *et al.* [Belle Collaboration], Phys. Rev. D 88, 114006 (2013), arXiv:1309.0704 [hep-ex].

[17] B. Pal *et al.* [Belle Collaboration], Phys. Rev. Lett. 116, 161801 (2016), arXiv:1512.02145 [hep-ex].

[18] M. Feindt, F. Keller, M. Kreps, T. Kuhr, S. Neubauer, D. Zander and A. Zupanc, Nucl. Instrum. Meth. A 654, 432 (2011), arXiv:1102.3876 [hep-ex].

[19] R. Glattauer *et al.* [Belle Collaboration], Phys. Rev. D 93, 032006 (2016), arXiv:1510.03657 [hep-ex].

[20] P. Hamer *et al.* [Belle Collaboration], Phys. Rev. D 93, 032007 (2016), arXiv:1509.06521 [hep-ex].